

Modeling magma flow and cooling in dikes: Implications for emplacement of Columbia River flood basalts

Heather L. Petcovic

Department of Geosciences, Western Michigan University, Kalamazoo, Michigan, USA

Josef D. Dufek

Department of Earth and Space Sciences, University of Washington, Seattle, Washington, USA

Received 15 September 2004; revised 23 May 2005; accepted 20 June 2005; published 1 October 2005.

[1] The Columbia River flood basalts include some of the world's largest individual lava flows, most of which were fed by the Chief Joseph dike swarm. The majority of dikes are chilled against their wall rock; however, rare dikes caused their wall rock to undergo partial melting. These partial melt zones record the thermal history of magma flow and cooling in the dike and, consequently, the emplacement history of the flow it fed. Here, we examine two-dimensional thermal models of basalt injection, flow, and cooling in a 10-m-thick dike constrained by the field example of the Maxwell Lake dike, a likely feeder to the large-volume Wapshilla Ridge unit of the Grande Ronde Basalt. Two types of models were developed: static conduction simulations and advective transport simulations. Static conduction simulation results confirm that instantaneous injection and stagnation of a single dike did not produce wall rock melt. Repeated injection generated wall rock melt zones comparable to those observed, yet the regular texture across the dike and its wall rock is inconsistent with repeated brittle injection. Instead, advective flow in the dike for 3–4 years best reproduced the field example. Using this result, we estimate that maximum eruption rates for Wapshilla Ridge flows ranged from 3 to 5 km³ d⁻¹. Local eruption rates were likely lower (minimum 0.1–0.8 km³ d⁻¹), as advective modeling results suggest that other fissure segments as yet unidentified fed the same flow. Consequently, the Maxwell Lake dike probably represents an upper crustal (~2 km) exposure of a long-lived point source within the Columbia River flood basalts.

Citation: Petcovic, H. L., and J. D. Dufek (2005), Modeling magma flow and cooling in dikes: Implications for emplacement of Columbia River flood basalts, *J. Geophys. Res.*, 110, B10201, doi:10.1029/2004JB003432.

1. Introduction

[2] The Miocene Columbia River magmatic event produced ~234,000 km³ [Camp *et al.*, 2003] of tholeiitic basalt to basaltic andesite lavas that flooded an extensive area of the northwestern United States (Figure 1). About two thirds of the Columbia River Basalt Group (CRBG) erupted in less than a million years as flows of Grande Ronde Basalt (~16.5–15.6 Ma [Baksi, 1989]). The Grande Ronde consists of more than 120 individual flows, many of which exceed 2500 km³ in volume and traveled more than 750 km from their vents [Reidel *et al.*, 1989], making them among the largest recognized terrestrial basalt flows.

[3] Emplacement rates and mechanisms of these large-volume flood basalts have been a matter of controversy. Early workers [Shaw and Swanson, 1970] suggested

emplacement as turbulent flows racing across the landscape in weeks to months. However, in analogy to inflated pahoehoe flows observed in Hawaii [i.e., Hon *et al.*, 1994], Self *et al.* [1996] suggested that Columbia River flood basalts were emplaced as large, inflated flow fields. Flow inflation occurs as centimeter-scale lobes of lava develop a chilled, viscoelastic skin, then expand with continued injection of fluid lava. Ho and Cashman [1997] found less than 0.04°C km⁻¹ of heat loss along the 500-km-long Ginko flow, suggesting either extremely rapid emplacement, or (more likely) emplacement under an insulating crust. Thordarson and Self [1998] described lobes and other inflation structures in the Roza basalt of the CRBG. Inflation is also consistent with compositional data; compositionally zoned Saddle Mountains Basalt [Reidel and Fecht, 1987; Reidel, 1998] and Grande Ronde Basalt [Reidel, 2005] flows have been described where progressively younger lava is preserved toward the center in a single cooling unit.

[4] Whereas flow inflation is recognized as a critical mechanism for flood basalt emplacement, controversy per-

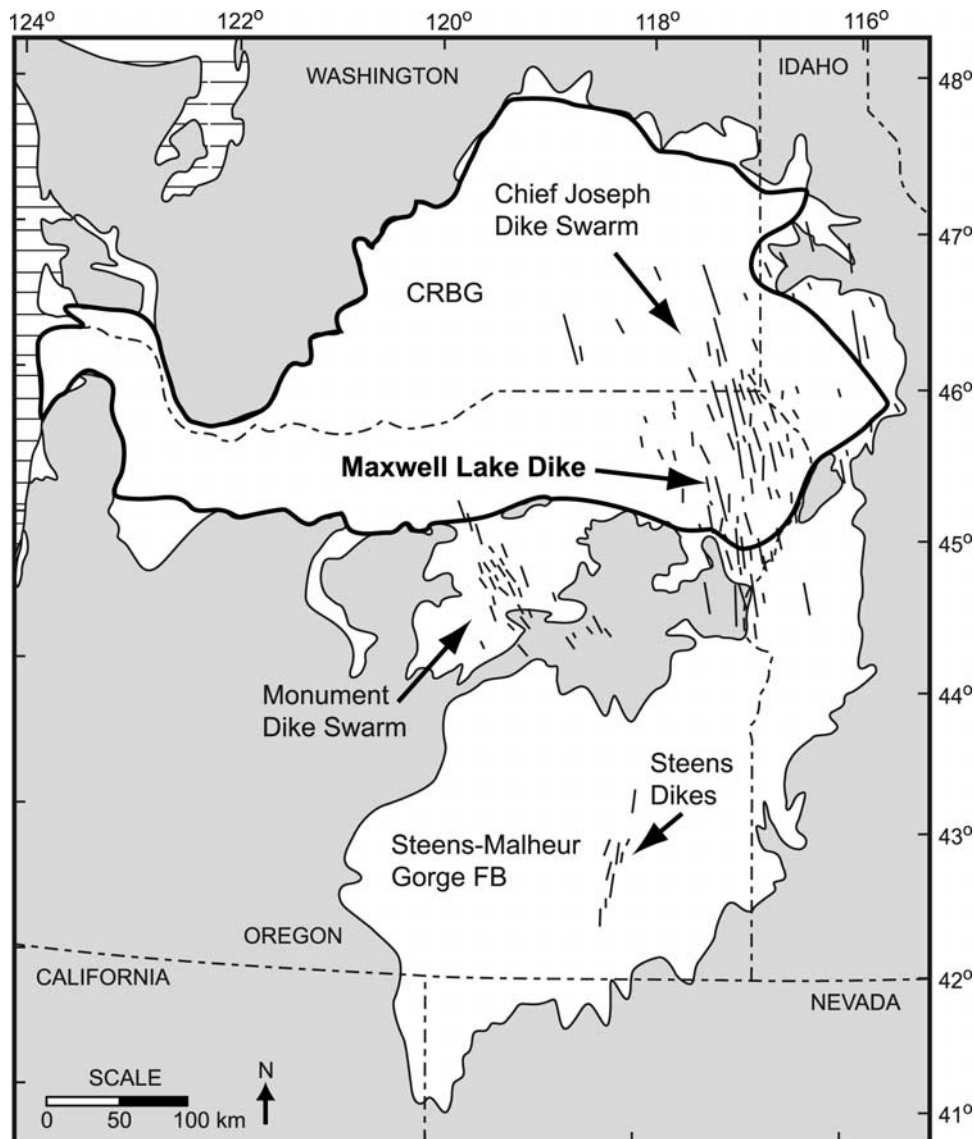


Figure 1. Location of the Maxwell Lake dike in the context of the Columbia River Flood Basalt Province. Unshaded area depicts the extent of the province, which consists of the Columbia River Basalt Group (CRBG) and Steens-Malheur Gorge flood basalts [after *Camp and Ross, 2004*]. Short lines indicate the approximate locations of feeder dikes [after *Tolan et al., 1989; Camp and Ross, 2004*]. Heavy black line shows the approximate extent of the member of Wapshilla Ridge [after *Reidel et al., 1989*].

sists over eruption and emplacement rates. Slow emplacement over years to a few decades is advocated in the CRBG based on conductive cooling models in the Roza [Thordarson and Self, 1998], and is supported by thermal models [Keszthelyi and Self, 1998]. Compositional data, however, is more consistent with eruption and emplacement over weeks to months. Reidel [1998, 2005] documented examples where two flows were preserved in individual dikes and vents, yet mixed together to form a single flow more than 200 km from the source, requiring rapid emplacement. Recently, *Petcovic and Grunder* [2003] concluded that a Grande Ronde dike could have fed flows for about 4 years based on the extent of melting reactions in the wall rock adjacent to the dike.

[5] Here, we explore thermal models of injection, flow, and cooling of basalt in the Maxwell Lake dike, a likely

feeder to the member of Wapshilla Ridge of the Grande Ronde Basalt. This dike caused partial melting in adjacent granitoid wall rock [Petcovic, 2000; *Petcovic and Grunder, 2003*]. The quenched partial melt zones adjacent to this dike preserve an integrated thermal record of heating during magma flow in the dike and cooling after flow ceased. Using the thermal models, we are able to place limits on the longevity of the dike, and therefore estimate eruption rates of the Wapshilla Ridge basalt.

2. Geological Constraints

[6] Nearly 75% of flood lavas in the CRBG were fed by the Chief Joseph dike swarm (Figure 1), in which as many as 20,000 dikes occur [Taubeneck, 1970]. The swarm strikes about N10°W; individual dikes dip within 30° of vertical

Table 1. Whole Rock Major and Trace Element Data for the Maxwell Lake Dike and Member of Wapshilla Ridge^a

	Maxwell Lake Dike		Member of Wapshilla Ridge ^b						
	MLT-01-65	MLR-01-72	C6827	C6828	C6829	C6830	SWEP87-A	SWEP87-B	WCHI18
	<i>Oxide, wt %</i>								
SiO ₂	53.74	53.54	54.33	55.23	54.72	55.29	55.50	53.40	55.12
TiO ₂	2.48	2.46	2.43	2.42	2.41	2.43	2.43	2.39	2.49
Al ₂ O ₃	13.33	13.14	13.70	13.52	13.42	13.79	13.56	14.01	13.95
FeO ^c	13.47	13.43	13.79	13.66	13.69	13.49	12.75	13.10	12.40
MnO	0.23	0.22	0.21	0.21	0.21	0.21	0.22	0.23	0.17
MgO	3.87	3.89	3.60	3.37	3.53	3.78	3.30	3.69	3.04
CaO	7.42	7.40	7.33	6.93	7.15	7.34	6.83	7.72	6.75
Na ₂ O	3.49	3.51	3.25	3.37	3.33	3.20	3.59	3.28	3.39
K ₂ O	1.45	1.48	1.50	1.72	1.67	1.57	1.87	1.63	1.83
P ₂ O ₅	0.42	0.41	0.41	0.41	0.40	0.41	0.41	0.43	0.48
Total	99.89	99.48	100.55	100.83	100.53	101.51	100.45	99.87	99.62
	<i>Trace Elements, ppm</i>								
Ni	9	12	6	3	8	7	2	6	7
Cr	26	26	30	26	32	35	21	29	29
Sc	38	37	33	29	30	34	27	30	29
V	398	401	434	406	432	422	407	431	400
Ba	608	587	620	658	640	600	653	547	696
Rb	34	34	45	49	47	45	52	38	50
Sr	328	321	321	311	315	317	317	340	324
Zr	203	201	183	189	183	175	193	185	195
Y	43	43	39	38	36	36	39	39	39
Nb	14	13	16	14	15	15	16	17	16
Ga	24	21	22	24	23	20	25	25	23
Cu	64	63	27	14	32	23	71	45	22
Zn	138	134	130	132	129	128	156	154	150

^aAll samples analyzed as bulk rock by XRF at Washington State University GeoAnalytical Laboratory.

^bData provided by S. P. Reidel, unpublished.

^cAll Fe reported as FeO.

and continue for 1–2 km along strike, often as en echelon segments [Taubeneck, 1970]. Most dikes are 7–10 m thick, though dikes as thin as 2 m and as thick as 50 m have been observed [Taubeneck, 1970]. Dikes are concentrated into clusters of 7–12 dikes per km², where each cluster probably represents an eruptive axis for CRBG volcanism [Taubeneck and Duncan, 1997]. The majority of dikes are chilled against their wall rock; however, rare dikes lack chilled margins and have induced partial melting in their wall rock. In such dikes, wall rock melt zones are up to one half as thick as the dike, and in cases where dikes are not vertical, the hanging wall has a thicker melted zone [Grunder and Taubeneck, 1997].

[7] We have examined a Grande Ronde dike hosted in biotite- and hornblende-bearing tonalite of the Wallowa Batholith. The Maxwell Lake dike (Figure 1) strikes N20°E, dips about 75°W, and continues in en echelon segments for at least one km along strike. Paleodepth at the time of dike emplacement was about 2 km [Petcovic and Grunder, 2003]. In the northern of two en echelon segments examined, the dike is 6–11 m thick where it is chilled against wall rock, and 11–15 m thick where it caused wall rock melting. Wall rock melt zones parallel to both dike margins continue for 85 m along strike, making up ~60% of the total length of dike exposed. In the southern en echelon segment, the dike is 3–8 m thick. Here, wall rock melt zones extend 55 m along strike and are as thick as 4 m, containing up to 47 vol % quenched melt produced by dehydration-melting reactions. Silicic melt (glass plus quench crystals) is localized around sites where biotite and hornblende were consumed, and as millimeter-thick

seams on residual plagioclase-quartz grain boundaries. Wall rock melt zones and melting reactions along the southern en echelon segment are described in detail elsewhere [Petcovic, 2000; Petcovic and Grunder, 2003].

[8] Direct connections between dikes, vents, and flows have been observed in only a few cases in the CRBG [Gibson, 1969; Swanson *et al.*, 1975; Swanson and Wright, 1981; Hooper and Reidel, 1989; Reidel and Tolan, 1992]. In the absence of direct dike-vent-flow connections, correlations have been established on the basis of compositional and paleomagnetic data [Price, 1977; Ross, 1983; Mangan *et al.*, 1986]. Compositional data have long been used to discriminate and correlate CRBG flows across the province [e.g., Hooper, 2000]. On the basis of available compositional data, we have made a preliminary correlation between the Maxwell Lake dike and the member of Wapshilla Ridge of the Grande Ronde Basalt (Table 1 and Figure 2). The Wapshilla Ridge is ubiquitously enriched in TiO₂ and P₂O₅ compared to nearly all other Grande Ronde units; given our current knowledge of compositional trends within the Grande Ronde, it is at present the best match for the Maxwell Lake dike (S. P. Reidel, personal communication, 2005).

[9] The member of Wapshilla Ridge is composed of as many as 8–10 flows of narrow though variable compositional range, and belongs to the R2 paleomagnetic interval of Grande Ronde volcanism (~15.5 Ma [Reidel *et al.*, 1989]). It is also widely distributed across the CRBG province (Figure 1), and is the most voluminous member of the Grande Ronde at an aggregate volume of ~50,000 km³ (S. P. Reidel, personal communication, 2004). Individual

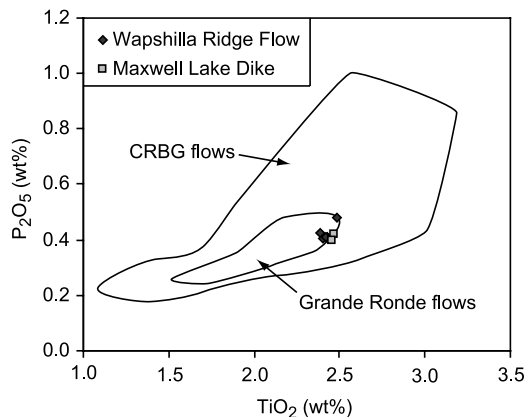


Figure 2. Plot of TiO_2 versus P_2O_5 for selected samples of the Maxwell Lake dike and member of Wapshilla Ridge. Both dike and flow samples plot at high TiO_2 and high P_2O_5 within the field for Grande Ronde flows. Additional bulk rock major and trace element data are provided in Table 1. Fields for CRBG and Grande Ronde flows are after Hooper and Hawkesworth [1993].

flows of the Wapshilla Ridge have not been examined in detail, but are commonly in excess of 2500 km^3 with some flows exceeding 5000 km^3 (S. P. Reidel, personal communication, 2004).

3. Thermal Modeling

[10] Two types of models were used to assess the development of wall rock melting as a consequence of basalt intrusion: conduction simulations and advection simulations. In a series of static conduction simulations, we varied the timing between dike injection(s) and duration of basalt flow in the dike in order to characterize development of wall rock melt zones using three end-member scenarios: instantaneous injection, repeated brittle injection, and sustained flow. In these simulations enthalpy was conserved in the dike and surrounding wall rock, which were assumed to have nonlinear melt fraction to temperature relations (Figure 3). As a proxy for sustained flow, the temperature inside the dike was held constant during the simulated duration of dike flow. The static conduction simulations were developed to explore a range of conditions that could have given rise to the observed wall rock melt zones; in particular, the simulation of sustained flow provided an upper bound to the temperature gradient at the dike/wall rock interface, as the temperature gradient in a flowing dike should decrease with time.

[11] In order to refine our initial calculations and determine magma flow rates in the dike, advective transport simulations were performed in which the conservation of momentum and continuity equations were explicitly used to determine the flow velocities in the developing dike system and the resulting influence on the transport of enthalpy. Vertical pressure gradients and buoyancy drove magma velocities in these simulations.

[12] In all simulations, a 10-m-wide dike at 1145°C (liquidus temperature) was instantaneously injected into 50°C tonalite wall rock. As depicted schematically in

Figure 4, the dike was assumed to be injected vertically. In the absence of field-measured flow direction indicators, vertical flow was assumed; however, similar results would be obtained for horizontal transport if a similar total pressure gradient were applied. Equations governing the simulations are given below, with symbols given in Table 2; further details of the solution procedure are presented by Dufek [2004] and Dufek and Bergantz [2005]. This approach uses a finite volume numerical method, with a predictor-corrector algorithm to compute the partitioning of enthalpy into sensible and latent heat during phase change processes for nonlinear melt fraction to temperature relationships. The numerical grid and boundary conditions are specified in Figure 4.

[13] One of the principal differences between this approach and previous calculations [Bruce and Huppert, 1990; Fialko and Rubin, 1999] is the incorporation of nonlinear melt fraction to temperature relationships specific to the magma/solid composition (Figure 3). In the advection simulations the melt fraction relationship can have an important effect on the multiphase viscosity. This can result in a “jelly sandwich” configuration (i.e., high melt fraction basalt in the interior of the dike, solidified basalt at the edge of the dike, molten wall rock adjacent to the dike, and finally solid wall rock at some distance from the dike), which may be very important in considering thermal and dynamic evolution of these dikes [Huppert and Sparks, 1989; Bergantz, 1990]. Shear heating [Fialko and Rubin,

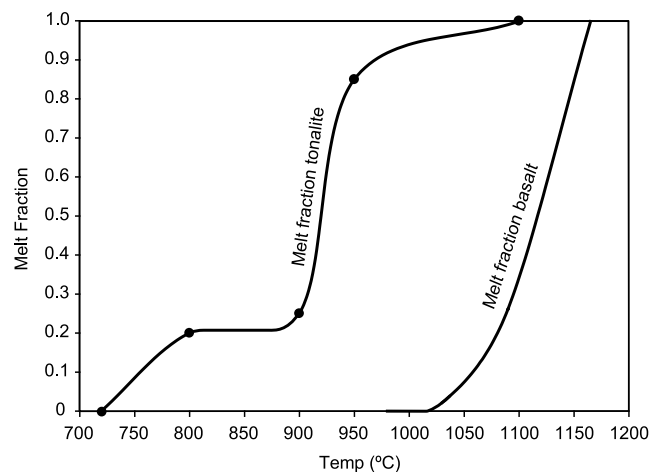


Figure 3. Melt fraction diagram for the Grande Ronde Basalt and tonalite wall rock. The melting curve for the basalt was generated using the MELTS program of Ghiorso and Sack [1995] supplemented with data from Marsh [1981]. The tonalite melting curve was generated from experimental data shown as dark circles from Pivinskii and Wyllie [1968], from their Tonalite 1213 Needle Point Pluton (mode, 55.1% plagioclase, 20.8% quartz, 12.1% biotite, 9.6% hornblende, 1.6% orthoclase, 0.5% Fe-Ti oxides and accessory phases). We chose this lithology because of its similar mode and bulk composition to the Wallowa tonalite (mode, 44.9% plagioclase, 19.5% quartz, 13.6% hornblende, 13.5% biotite, 7.5% orthoclase, 1.1% Fe-Ti oxides and accessory phases; for additional data, see Petcovic and Grunder [2003]).

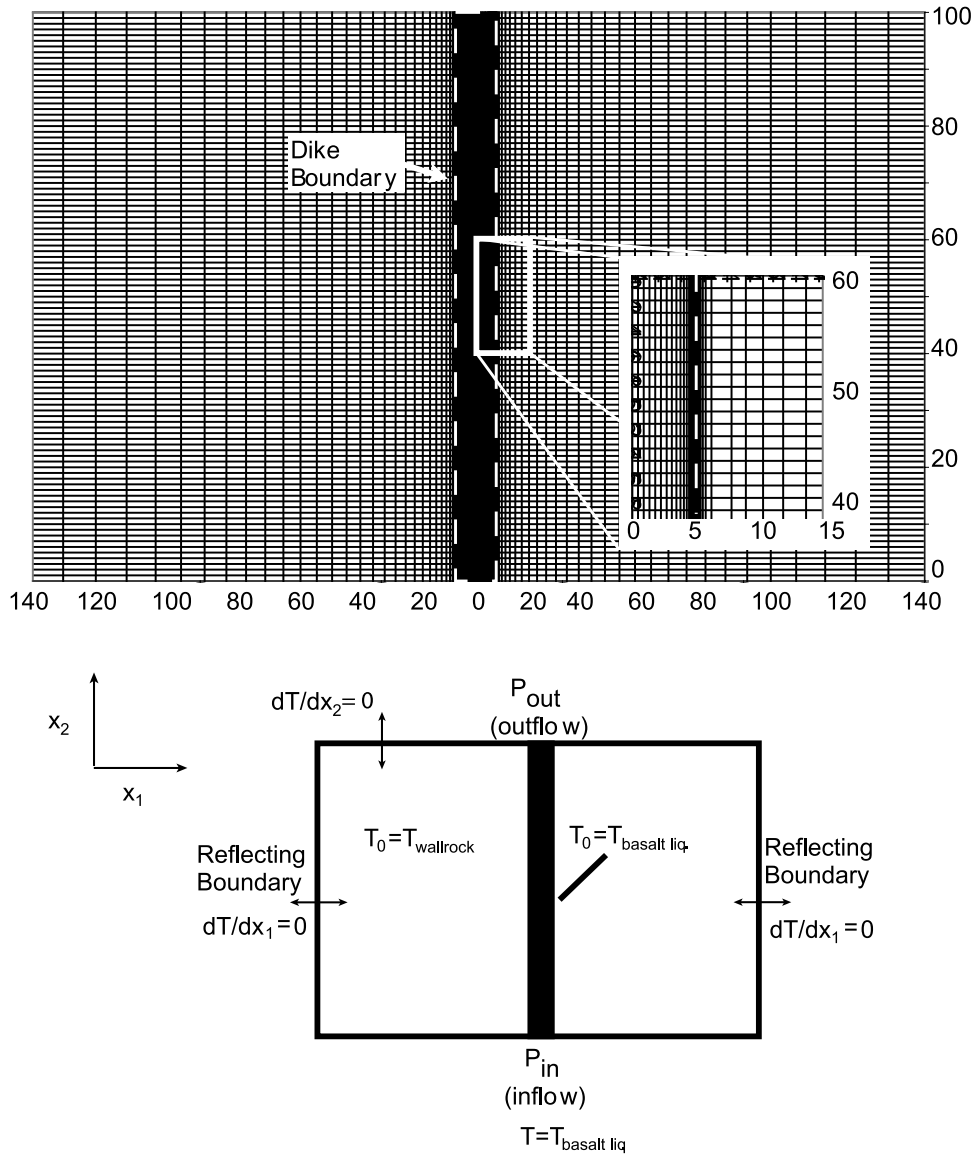


Figure 4. Numerical grid and boundary conditions used in all diking simulations (static conduction simulations and advective flow simulations). Note that the numerical grid is refined in the vicinity of the dike boundaries.

1999] was not explicitly considered in these simulations, although its potential impact is evaluated in the model results section.

3.1. Model Formulation: Conduction Simulations

[14] In the static conduction simulations, conservation of enthalpy (equations (1) and (2)) was solved. In order to close the conservation of enthalpy equation (equation (1)) the melt fraction must be given as a function of temperature (Figure 3). Because of the assumed vertical orientation of the dike in these simulations and the associated symmetry, thermal gradients only developed perpendicular to the dike orientation (i.e., variation is 1-D). The simplified equation for conservation of enthalpy is

$$\frac{\partial H}{\partial t} = \frac{\partial}{\partial x_1} k_{mix} \left(\frac{\partial}{\partial x_1} T \right), \tag{1}$$

where

$$H = \rho_{mix} \int_{T_{ref}}^T c_{mix} dT + \rho_{mix} fL, \tag{2}$$

where the first term on the right-hand side is sensible heat and the second term is latent heat.

3.2. Model Formulation: Advection Simulations

[15] Vertical pressure gradients and buoyancy can both cause magma to rise from depth, and to explicitly model this process the full set of conservation equations for enthalpy, momentum, continuity, and chemical species equation must be solved. The conduction simulation enthalpy equation (equation (1)) was modified to include two-

Table 2. Symbols and Values Used in Modeling

Symbol	Parameter	Numerical Value	Units
H	enthalpy		J
t	time		s
k	thermal conductivity	3.0 (tonalite) ^a 1.7 (basalt) ^a	W (m K) ⁻¹
c	heat capacity	1100.0 (tonalite) ^a 1150.0 (basalt) ^a	J (kg K) ⁻¹
T	temperature		K
f	melt fraction		
L	latent heat	1 × 10 ⁵ (tonalite) ^b 1 × 10 ⁵ (basalt) ^b	J kg ⁻¹
l_m	Prandtl mixing length		m
g	gravitational acceleration	9.8	m s ⁻²
v_i	velocity		m s ⁻¹
D	average chemical diffusivity	10 ⁻¹¹ (melt) ^c	m ² s ⁻¹
S	shear heating		J (m ² s) ⁻¹
μ_m^i	melt dynamic viscosity	from <i>Shaw</i> [1972] with crystal correction	Pa s
μ_t	turbulent viscosity		Pa s
ρ_c	wall rock melt density	2300	kg m ⁻³
ρ_c^s	wall rock solid density	2650 ^c	kg m ⁻³
ρ_b	basalt melt density	2600 ^c	kg m ⁻³
ρ_b^s	basalt solid density	2800 ^c	kg m ⁻³

^a*Touloukian et al.* [1981].^b*Barboza and Bergantz* [1996].^c*Dobran* [2001].

dimensional effects and the advection term (symbols given in Table 2):

$$\frac{\partial H}{\partial t} + \frac{\partial}{\partial x_j} (v_j H) = \frac{\partial}{\partial x_i} k_{\text{mix}} \left(\frac{\partial}{\partial x_i} T \right). \quad (3)$$

The continuity, momentum, and chemical species equations are given by

$$\frac{\partial v_j}{\partial x_j} = 0, \quad (4)$$

$$\frac{\partial}{\partial t} (\rho_{\text{mix}} v_i) + \frac{\partial}{\partial x_j} (\rho_{\text{mix}} v_j v_i) = - \frac{\partial P}{\partial x_i} + \mu_{\text{mix}} \frac{\partial^2 v_i}{\partial x_j^2} + \rho_{\text{mix}} g, \quad (5)$$

$$\frac{\partial \gamma}{\partial t} + \frac{\partial}{\partial x_j} (v_j \gamma) = \frac{\partial}{\partial x_i} D \left(\frac{\partial}{\partial x_i} \gamma \right), \quad (6)$$

respectively. Einstein summation is implied for the previous set of equations. The set of equations as given here implies incompressible, laminar flow. The Maxwell Lake dike lacked evidence of extensive volatile exsolution (less than 1% vesicles), and hence the incompressible assumption should be valid for these conditions. In order to consider the potential for turbulent flow, we also conducted simulations using a Prandtl mixing length model which introduced a turbulent viscosity (μ_t) in addition to the magmatic viscosity:

$$\mu_t = \rho l_m^2 \left| \frac{\partial v_i}{\partial x_j} \right|. \quad (7)$$

To close the model, we used the mixing length (l_m) parameterization developed for fully developed pipe and channel flow [*Rodi*, 1984]:

$$l_m = L \left[0.14 - 0.08(1 - y/L)^2 - 0.06(1 - y/L)^4 \right]. \quad (8)$$

However, a posteriori examination of the laminar results show that for reasonable pressure gradients the Reynold's number was $<10^3$ using the mixture (melt plus solid) viscosity for these dikes and they likely did not become fully turbulent. This is consistent with field evidence in the Maxwell Lake dike, whose ~ 10 m thickness is considerably less than the dike thicknesses predicted in other turbulent calculations that caused extensive melt back [i.e., *Fialko and Rubin*, 1999]. Furthermore, since the solidus of the dike was elevated relative to the solidus of the wall rock, crystallization was typically induced at the dike margin, which considerably increased the viscosity of the basaltic material. As will be examined later, this altered the velocity profile from plane Poiseuille flow and increased velocity gradients at the margins of the flow similar to the mean velocity profile observed in turbulent flows. Although similar velocity profiles were observed, the crystal plus melt viscosity may be considerably larger than the effective turbulent viscosity; therefore turbulence, under these specific conditions, may not be as important as the contribution to the viscosity due to phase change.

[16] The gradient of magmatic overpressure was specified as 75 Pa m⁻¹. The presence of magmatic overpressure assumes a pressurized magma reservoir at depth. This overpressure is bounded by rock yield strength [*Dobran*, 1992], and was selected so that flow was maintained in the dike for the ~ 4 -year timescales predicted in the conduction parametric study. Both this overpressure and magma buoy-

ancy will cause the magma to rise from depth. For the density difference of 50 kg m^{-3} between the basaltic magma and tonalite wall rock, this gives a total equivalent pressure gradient (buoyancy plus overpressure) of 565 Pa m^{-1} . While we assume vertical transport in these simulations, similar results would be obtained for horizontal dike propagation if a similar total driving force was applied.

3.3. Constitutive Relations

[17] As material is being advected and cooled, it is possible for mixtures of materials to be inside any given model control volume (melt plus crystals and basalt plus wall rock, for instance). To implement the control volume simulations, the thermal and physical transport properties of the system were developed as volume-weighted mixtures of material properties using local composition and melt fraction parameters. A composition parameter, γ , describes the volume fraction of wall rock material or intruded basalt residing at a particular location. If the γ equals one, the region is all wall rock, and if it equals zero it is all basalt. Intermediate values indicate relative proportions, and hence locally mixed material. The variable f denotes the local melt fraction. In the following nomenclature, the subscripts b and t refer to properties of the basalt and tonalitic wall rock, respectively. Superscripts s and l refer to solid and melt. The mixture density, heat capacity, and conductivity are defined as (symbols given in Table 2),

$$\rho_{\text{mix}} = \gamma f_t \rho_t^l + \gamma (1 - f_t) \rho_t^s + (1 - \gamma) f_b \rho_b^l + (1 - \gamma) (1 - f_b) \rho_b^s, \quad (9)$$

$$c_{\text{mix}} = \gamma f_t c_t^l + \gamma (1 - f_t) c_t^s + (1 - \gamma) f_b c_b^l + (1 - \gamma) (1 - f_b) c_b^s, \quad (10)$$

$$k_{\text{mix}} = \gamma f_t k_t^l + \gamma (1 - f_t) k_t^s + (1 - \gamma) f_b k_b^l + (1 - \gamma) (1 - f_b) k_b^s, \quad (11)$$

respectively.

[18] Crystal and melt mixtures below a critical melt fraction of 0.4 were assumed rigid in these simulations. This is approximately the melt fraction at which an interlocking crystalline framework forms for a monodisperse crystal size distribution [Scaillet *et al.*, 1998], and does not treat complications arising from other crystal size distributions or background strain rate. To model a rigid wall rock, the viscosity of the wall rock was assumed sufficiently high ($>10^{20} \text{ Pa s}$) so that no motion of the wall rock was possible over the relatively short duration of these simulations (1–10 years). Above the critical melt fraction, the mixture viscosity was modified from the melt viscosity to account for the macroscopic effect of increased drag between crystals and melt [Marsh, 1981; Dingwell *et al.*, 1993; Scaillet *et al.*, 1998; Dobran, 2001].

$$\mu_{\text{mix}} = \mu_m^i \left[1 + .75 \left(\frac{(1-f)/(1-\text{CMF})}{1-(1-f)/(1-\text{CMF})} \right) \right]^2. \quad (12)$$

The viscosity parameterization of Shaw [1972] was used to calculate the viscosity of the melt. With the crystal plus

magma mixture approach, dispersive-pressure segregation of crystals from the melt cannot be discerned. However, the complimentary conduction simulations present an end-member scenario in which the interior of the dike has constant temperature during dike flow (i.e., no crystallization is assumed during dike flow). This end-member is equivalent to complete removal of crystals in the dike during flow due to various segregation processes.

3.4. Model Sensitivity

[19] The model is sensitive to variations in the thermal parameters (density, heat capacity, and thermal conductivity) of the basalt and tonalite wall rock. In order to establish the combined effect of varying these parameters, we varied effective thermal diffusivity by factors of 0.1, 0.5, 2, and 10. For each value, static conduction simulations were conducted for 800 days of sustained flow in the dike. On the basis of comparison to other studies [e.g., Touloukian *et al.*, 1981], we conclude that varying the thermal diffusivity by a factor of 2 is a conservative estimate of model error. Varying the diffusivity by a factor of 2 created $\pm 22\%$ as much melt as the initial scenario, and wall rock melting was initiated in 17–64 days under the static conduction scenario.

4. Model Results

4.1. Static Conduction: Instantaneous Injection

[20] Injection of basalt without subsequent flow in a single, 10-m-thick dike was incapable of raising tonalite wall rock to its solidus temperature of $\sim 725^\circ\text{C}$ and therefore cannot generate wall rock melt (Figure 5), as noted elsewhere [e.g., Delaney, 1987]. We also explored the thermal effects of preheating the wall rock via prior dike injection; in this scenario, a 10-m-thick dike was first injected parallel to and 100 m east of the Maxwell Lake dike, a geometry observed in the field. The thermal energy of the first injection was insufficient to cause wall rock melting adjacent to the Maxwell Lake (second) injection. These results indicate that the production of wall rock melt required repeated injection or sustained flow.

4.2. Static Conduction: Repeated Brittle Injection

[21] Two or more injections of basalt at the same orientation in the dike were capable of generating wall rock melt zones. Two injections of magma without subsequent flow generated up to 22 vol % tonalite melt in zones as thick as 2 m (Figure 6), which is about half the amount and thickness of wall rock melt observed at the Maxwell Lake dike. By employing three or four injections, we reproduced the Maxwell criteria; for example, four injections each separated by ~ 1400 days generated up to 45 vol % melt in tonalite wall rock up to 5 m from the contact (Figure 6). In all cases, wall rock melting was maximized when the timescale of basalt intrusion approached the timescale of thermal diffusion [Petford and Gallagher, 2001], in this case about 200 days apart.

[22] Repeated brittle injection should result in the formation of internal chilled margins, such as those observed in compound or sheeted dikes. Whereas the Maxwell Lake dike has cross cut and eroded the chilled basalt at its margins, there is no textural evidence for

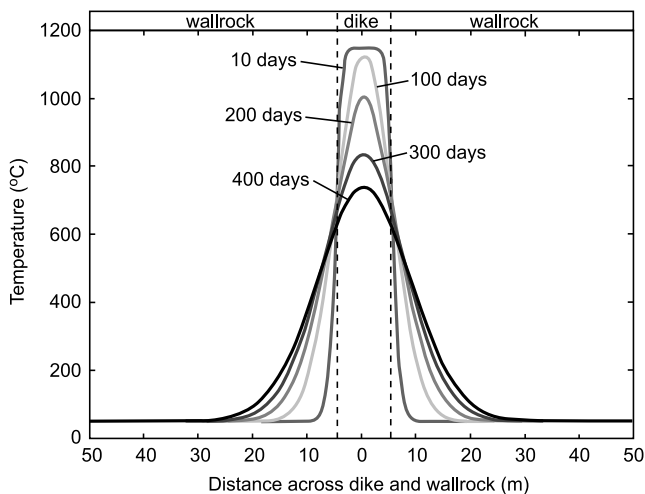


Figure 5. Results of the static conduction simulation for instantaneous injection followed by stagnation and cooling of a 10-m-thick dike. Isotherms are labeled in days of cooling following injection. Note that the wall rock adjacent to the dike never reaches its solidus ($\sim 725^{\circ}\text{C}$).

multiple, internal chilled margins. However, other CRBG dikes have been reported that lack internal chilled margins, but, based on fine-scale compositional variation within the dikes and/or flow distribution patterns, clearly fed multiple eruptions emplaced several months to years apart [e.g., Hooper, 1985; Reidel and Fecht, 1987; Reidel, 1998]. While we did not sample the Maxwell Lake dike at high enough density to completely rule out the possibility of repeated use, we conclude based on the available textural data that repeated brittle injection was unlikely to have produced the observed wall rock melt zones.

4.3. Static Conduction: Sustained Flow

[23] Simulating 4 years of basalt flow in the dike produced 5–30 vol % melt in wall rock up to 5 m from the contact, and up to 85 vol % wall rock melt adjacent to the dike (Figure 7). Melting of wall rock was initiated after about 30 days of flow; melting took place both during basalt flow in the dike, and during the first 2 years of cooling (Figure 7a). Wall rock reached its solidus temperature within about 4 years after basalt flow ceased. In comparison to the field data, the static conduction scenario produced wall rock melt zones of similar thickness and melt distribution, yet much higher melt fractions than observed (maximum 85 vol % versus 47 vol % melt observed in the Maxwell Lake dike).

[24] To place limits on the sustained flow end-member scenario, we also held the dike at its liquidus temperature for 1, 3, and 10 years prior to cooling. Sustained flow in the dike for 1 year produced wall rock melt zones 2.5 m thick with up to 45 vol % wall rock melt, whereas sustained flow for 3 years generated melt zones 4 m thick with up to 85 vol % melt. Ten years of sustained flow resulted in wall rock melt zones 9 m thick with a maximum of 85 vol % wall rock melt adjacent to the dike. On the basis of wall rock melt

zone thickness, 3–4 years of sustained flow produced the best fit to the Maxwell criteria.

4.4. Advective Transport

[25] The sustained flow static conduction simulation provided a first approximation of dike longevity, and was useful for providing a maximum temperature gradient at the dike/wall rock interface. The advective transport simulations, which consider magma viscosity and velocity effects in addition to simple conductive heating and cooling, were developed as a more realistic approximation of the conditions of magma flow.

[26] Model results suggest that 4 years of basalt flow in the dike produced <1–40 vol % melt in wall rock up to 5 m from the dike/wall rock contact (Figure 8). Wall rock melting was initiated after 320–380 days of flow, and wall rock had dropped below its solidus temperature within 2 years after flow ceased (Figure 8a). In this scenario, the maximum wall rock melt fraction as well as the thickness and distribution of wall rock melt zones closely approximates our field observations. Rapid cooling is supported by preservation of glass and the development of quench crystals in Maxwell Lake dike wall rock melt zones.

[27] After the initiation of dike flow, the margins of the dike solidified, thereby reducing the effective thickness of the mobile basalt and greatly increasing the viscosity of the melt plus crystal mixture near the solidified margins (Figure 9a). The initial centerline velocity was approximately 10 m s^{-1} , but rapidly decreased as the dike constricted and the mixture viscosity increased (Figure 9b). The dike reached maximum constriction after about 60 days of

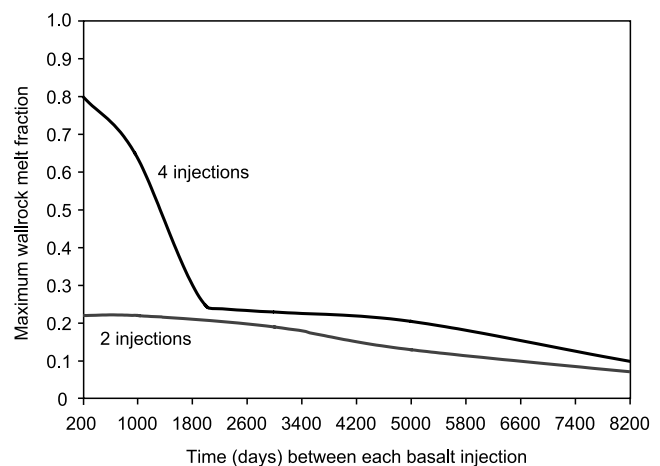


Figure 6. Results of the static conduction simulation for repeated brittle injection and stagnation in a 10-m-thick dike. Maximum tonalite wall rock melt fraction is plotted versus time between each basalt injection for the case of two and four injections. Each injection was instantaneous and, in the case of four injections, occurred at equal time intervals. The dramatic break in slope on the four injection curve is related to the form of the melt fraction curve for the tonalitic wall rock (Figure 3). Two hundred days was the lower limit of brittle failure criteria for the model, which required that the first pulse of magma solidified completely before the subsequent pulse(s) was (were) injected.

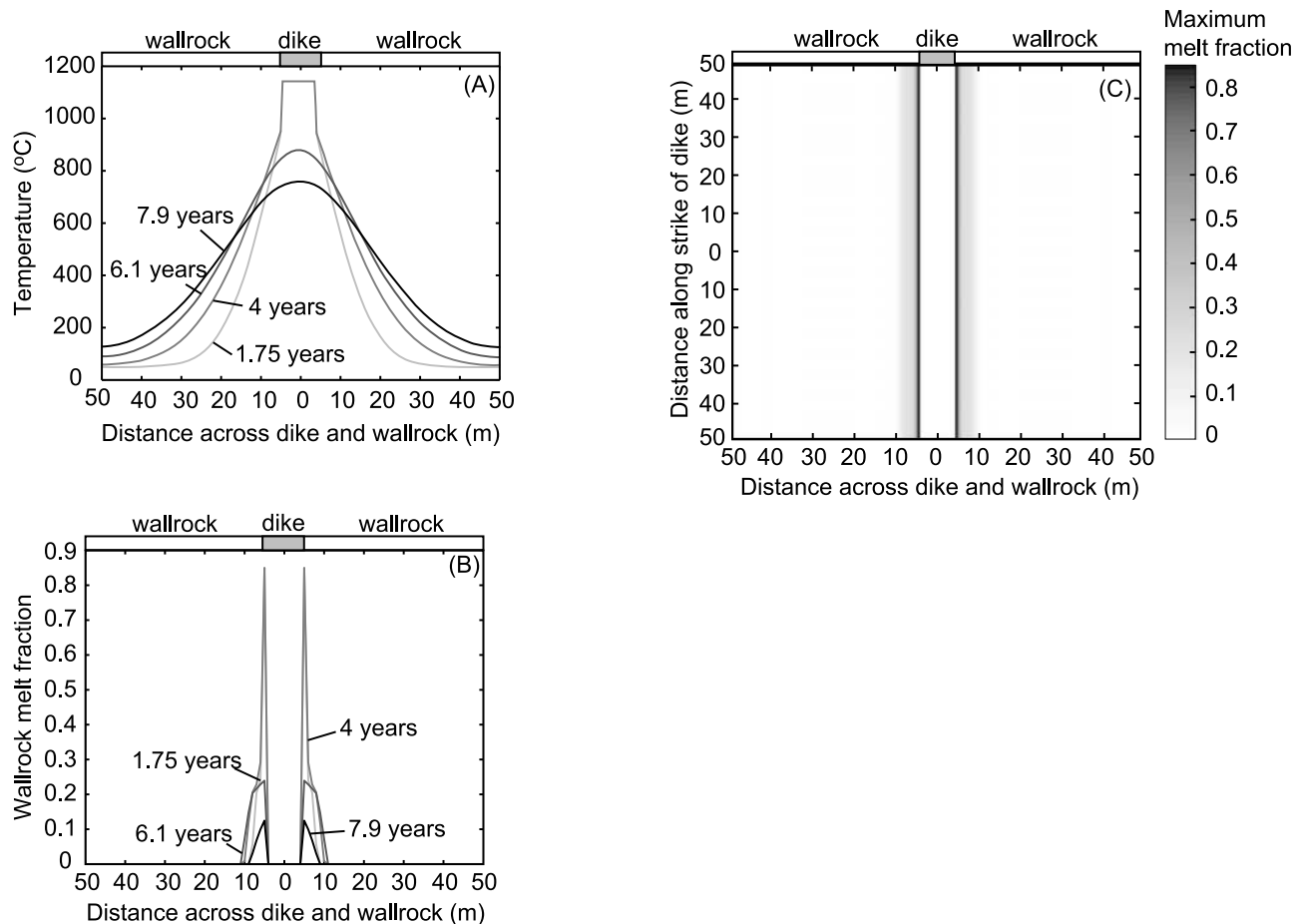


Figure 7. Results of the static conduction simulation modeling sustained flow for 4 years in a 10-m-thick dike. In the simulation, the region representing the dike was held at its liquidus temperature for 4 years, conductively heating and inducing partial melting in the adjacent wall rock region. After 4 years, both dike and wall rock were allowed to cool. The dike completely solidified after about 2 years of cooling. (a) Temperature versus distance across dike and wall rock both during flow and after basalt flow has ceased. Isotherms are labeled with years since the initiation of flow, with flow in the dike ceasing after 4 years. (b) Stepwise development of partial melt zones in wall rock during flow and after flow had ceased in the dike, isotherms labeled as in Figure 7a. (c) Plan view of dike and wall rock depicting time-integrated extent of partial melt zones in tonalite wall rock. Melting was initiated in wall rock after about 30 days of flow and continued for up to about 2 years after flow ceased, with wall rock dropping below its solidus temperature after about 4 years.

flow, accompanied by a minimum in the flux of basalt in the dike (Figure 10a). After the initial solidification, continued flow produced a small amount of melting in the previously solidified dike region, a phenomenon termed the thermal turnaround [Bruce and Huppert, 1990]. After the thermal turnaround, the basalt flux increased slightly (Figure 10a), although the average centerline velocity did not vary significantly from 2 m s^{-1} over the 4-year duration of dike flow (Figure 9b), suggesting these conditions produced a near steady state dike thickness.

[28] In comparison to the static conduction sustained flow scenario, the advective transport simulation generated lower wall rock melt fractions over the same duration of basalt flow. Temperatures within the dike and adjacent wall rock remained cooler in the advective transport simulation, and both the dike and wall rock cooled more rapidly after flow ceased. During the advective transport simulation, the

solidified dike margins insulated the system from the high-temperature gradients that were imposed in the conduction simulations. Although the dike margin solidified, near-solidus conditions were maintained for the duration of flow, which may explain why grain size is relatively uniform across the Maxwell Lake dike.

4.5. Comparison to Other Studies

[29] Insight into the importance of several modeling assumptions can be gained by comparing the results of this study with others that have examined basaltic dike systems. Our conduction simulations are qualitatively similar to previous models of dike–wall rock interaction using conduction as the heat transfer mechanism [e.g., Kitchen, 1989; Philpotts and Asher, 1993]. In these studies, prolonged magma flow in the dike was required for wall rock melting, which was initiated in 10–50 days. Like these previous

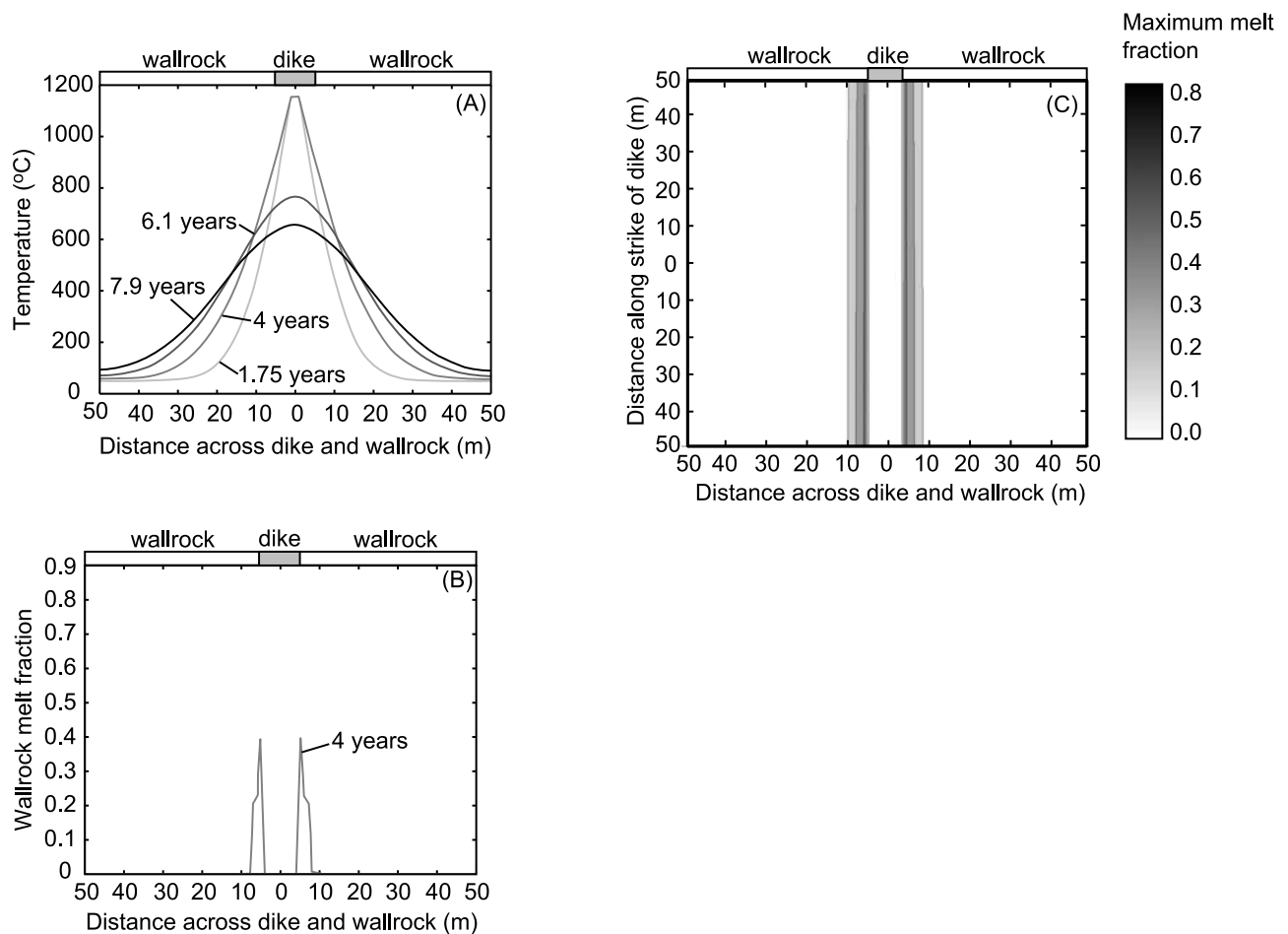


Figure 8. Results of the advective transport simulation, in which vertical basalt flow in the 10-m-thick dike was initiated by magmatic overpressure and sustained by buoyancy-driven flow for 4 years. Heat loss to the wall rock drove crystallization in the dike, and flow was impeded when the dike reached 40% crystallization. (a) Temperature versus distance across dike and wall rock during flow and after basalt flow has ceased. Isotherms are labeled with years since the initiation of flow, with flow in the dike ceasing after 4 years. (b) Maximum melt fraction developed in wall rock partial melt zones after dike flow has ceased. (c) Plan view of dike and wall rock depicting time-integrated extent of partial melt zones in tonalite wall rock. In this scenario, wall rock drops below its solidus temperature within 2 years after basalt flow ceased.

studies, our suite of conduction simulations assumed that the dike temperature was maintained at the liquidus while the dike was active. This assumption overpredicts the temperature gradient at the edge of the dike and, in our simulations, overpredicted wall rock melting, especially immediately after dike intrusion.

[30] Additional work has sought to improve on the conduction results by examining the role of advection in dike-wall rock interaction. For example, *Bruce and Huppert* [1990] modified the model of *Delaney and Pollard* [1982] to incorporate laminar Poiseuille flow in their solution. They noted that there was a critical dike thickness (1–2 m for wall rock initially 0°C and driving pressure gradients of 2000 Pa m⁻¹) below which dikes would eventually freeze and above which melt back eventually occurred. *Fialko and Rubin* [1999] extended the analysis to consider the effect of turbulence and shear heating. In their calculations, if the Reynolds number exceeded 2000 (i.e., the onset of turbulence in their

model) the melt back would be further enhanced due to cross-stream advection. This enhanced melt back could produce dike thicknesses over an order of magnitude larger than their original thicknesses. Both the *Bruce and Huppert* [1990] and *Fialko and Rubin* [1999] simulations considered the case of isoviscous magma, and assumed that the wall rock and dike had a common solidus, liquidus, and linear melt fraction to temperature relationships.

[31] To build upon this work, we incorporated melt fraction to temperature relationships appropriate for a tonalitic wall rock and basaltic magma (Figure 3) and used a rheology that incorporated the effect of crystallization. The viscosity gradients in the dike that developed due to crystallization caused the flow profiles to deviate from the parabolic profiles expected for isoviscous Poiseuille flow. The resulting temperature (Figure 8a) and velocity (Figure 9b) profiles across the dike have smaller gradients near the centerline, similar to those predicted in turbulent flows [*Fialko and Rubin*, 1999]; however extensive melt

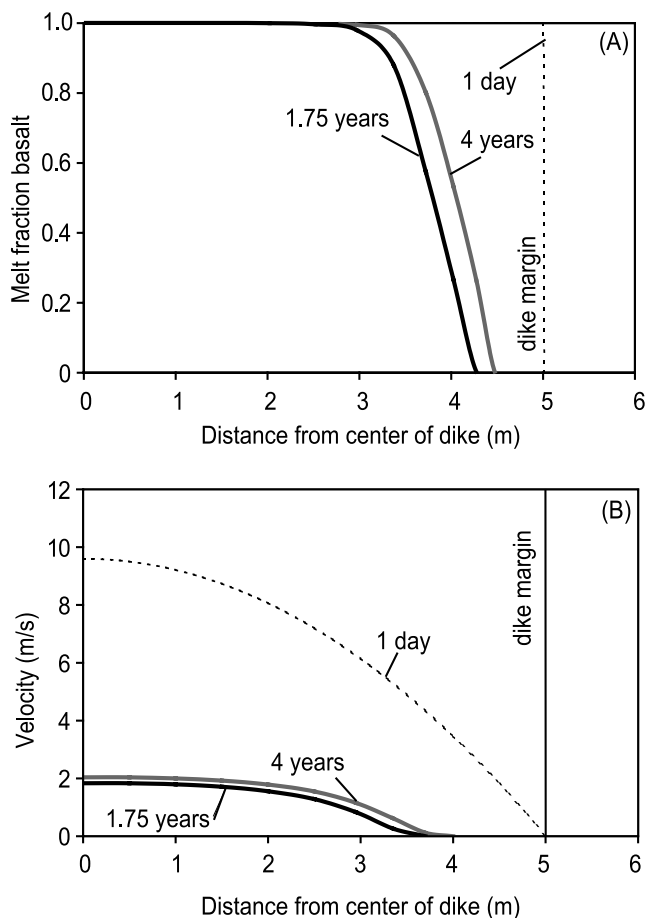


Figure 9. Advective transport simulation results depicting solid-liquid processes affecting the dike margin. (a) Development of solidified basalt at the margin of the dike over the 4-year period while the dike was active. Isotherms are labeled as time after the initiation of flow in the dike. After 4 years, the solidified zone ($>40\%$ crystallization) is about 1 m thick, resulting in a “jelly sandwich” effect of liquid basalt at the dike center, ~ 1 m of solidified basalt at the dike margin, ~ 5 m of partially melted wall rock, and solid wall rock. (b) Velocity of basalt in the dike over the 4-year period that the dike was active, isotherms labeled as in Figure 9a. Magma velocity drops rapidly and reaches a steady state of about 2 m s^{-1} after about 60 days of flow.

back and high Reynolds numbers were not observed in our simulations. Our highest Reynolds number occurred at the beginning of the simulations and was approximately 1400 (using the average velocity in the dike), which approaches the chaotic advection-transition to turbulence regime but is likely well below the Reynolds numbers sufficient for fully developed turbulence [Pope, 2000]. Within 60 days of the onset of flow, the mixture viscosity increased, the average velocity decreased (Figure 9b), and during most of the 4-year duration of flow the Reynolds number was 10^1 – 10^2 . Although turbulence would be unlikely at these Reynolds numbers, a simple Prandtl mixing length model (equations (7) and (8)) was used to compare effective

turbulent viscosity to magmatic viscosity and to access whether the higher initial Reynolds numbers conditions might lead to the emergent onset of turbulence. Many turbulence models are most appropriate for fully developed turbulence, and our usage of the Prandtl mixing length model is not intended as a detailed analysis of the chaotic advection regime. However, incorporation of the mixing length model in the simulations produced negligible differences in the flow profiles, and given the low Reynolds number for most of the flow duration, more sophisticated turbulence models were not deemed necessary.

[32] The lack of development of turbulence in our simulations is consistent with the results of *Fialko and Rubin* [1999], who predicted that the transition to turbulent flow and rapid melt back would require dikes greater than 11 m thick and a viscosity of 50 Pa s. Our advection simulations had crystal plus melt viscosity greater than 50 Pa s; therefore greater critical dike thicknesses would be necessary to produce rapid melt back. It is unlikely that the Maxwell Lake dike started as a much thinner dike and grew

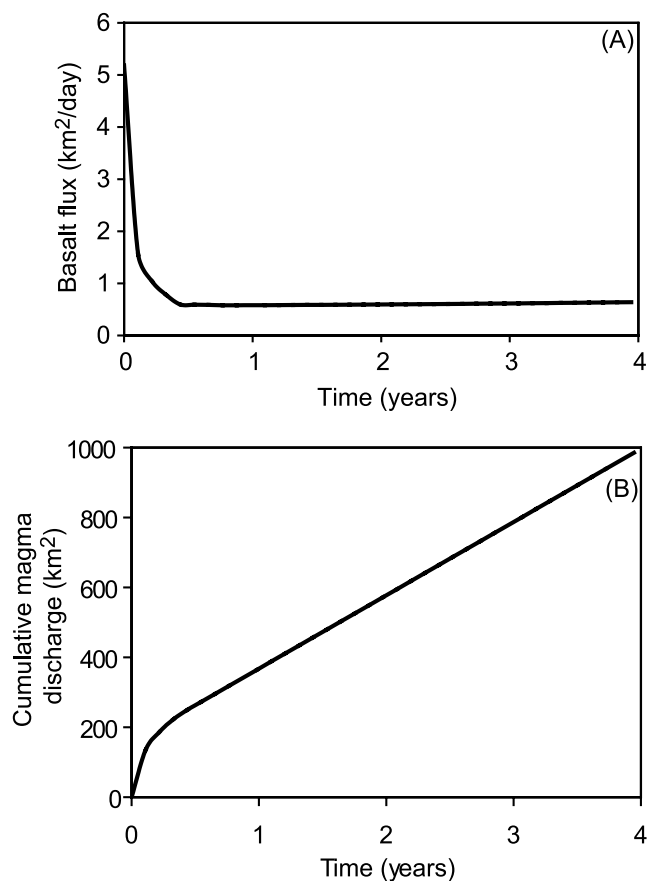


Figure 10. Basalt flux over 4 years of dike flow as calculated from the advective transport simulation. Flux is reported as $\text{km}^2 \text{ d}^{-1}$ for the two-dimensional simulations. (a) Initially high basalt flux decreasing rapidly as the margins of the dike solidify and the viscosity increasing due to crystallization. After ~ 60 days, previously solidified dike material begins to melt, slightly increasing basalt flux. (b) Total flux in Figure 10a integrated over time to give the cumulative magma discharge over the 4-year duration of dike flow.

by turbulent melt back to the outcrop thickness, as thinner dikes would have even smaller Reynolds numbers. However, the rare 30- to 50-m-thick dikes observed in parts of the Chief Joseph dike swarm may have experienced extensive melt back as predicted by *Fialko and Rubin* [1999].

[33] In order to estimate the error introduced by not assessing shear heating explicitly, we determined the shear heating profile after 4 years of flow. At this time, the velocity gradient near the edge of the flow was large and the viscosities were also high. Shear heating is given by (symbols given in Table 2)

$$S \approx \mu \left(\frac{\partial v_2}{\partial x_1} \right)^2 \quad (13)$$

for the flow configuration depicted in Figure 4 [*Fialko and Rubin*, 1999]. Whereas the maximum contribution due to latent heat reached nearly $1500 \text{ J (m}^3 \text{ s)}^{-1}$, the maximum contribution due to shear heating was about $150 \text{ J (m}^3 \text{ s)}^{-1}$, which may have had an effect comparable to the average latent heat in portions of the flow that were cooling slowly. During the initial stages of flow (approximately first 60 days), shear heating and latent heat release were both concentrated at the margins of the dike, and inclusion of shear heating would be equivalent to increasing the latent heat by a factor of 10–15%.

5. Implications for CRBG Flow Emplacement

[34] On the basis of compositional data, the Maxwell Lake dike was likely a feeder to one or more flows of the Wapshilla Ridge unit of the Grande Ronde Basalt (Table 1 and Figure 2). Results of the simulations allow us to estimate limits for the eruption rates of this flow. Assuming that the Maxwell Lake dike fed a typical Wapshilla Ridge flow of 5000 km^3 over a period of 3–4 years yields an average eruption rate of $3\text{--}5 \text{ km}^3 \text{ d}^{-1}$ ($\sim 40,000\text{--}50,000 \text{ m}^3 \text{ s}^{-1}$) (Table 3), which is a maximum estimate. The advective transport simulation provides a minimum estimate of basalt flux in the dike. The two-dimensional advection simulations calculated an area per time flux (Figure 10); to convert this to a volume flux, we assumed that flow was localized along the portions of the Maxwell Lake dike with partially melted wall rock margins (a cumulative length of about 150 m). This assumption yields an initial basalt flux of about $0.8 \text{ km}^3 \text{ d}^{-1}$ ($\sim 9000 \text{ m}^3 \text{ s}^{-1}$) waning rapidly to a sustained flux of about $0.1 \text{ km}^3 \text{ d}^{-1}$ (as converted from the area flux given in Figure 10a). However, cumulative magma discharge under this scenario produced a total flow volume of only 150 km^3 over 4 years (as converted from Figure 10b). Clearly, other fissure segments must have fed the same flow in order to produce a $2500\text{--}5000 \text{ km}^3$ cumulative volume typical of Grande Ronde flows.

[35] On the basis of the distribution of the Wapshilla Ridge unit, the dike-fissure system was at least 100 km long (S. P. Reidel, personal communication, 2004). In historical basalt eruptions (e.g., Laki 1783, Mauna Loa 1985), the entire fissure system was not active simultaneously. Instead, eruptive activity migrated along the length of the dike-fissure system, with each segment active for short

periods. For example, *Self et al.* [1997] suggest that fissure segments 4 km long were each active for ~ 3 months along the 150-km-long Roza system. The dike-fissure-vent system for the Wapshilla Ridge unit is yet poorly understood, and the existence of additional dike segments has not been determined. However, if additional fissure segments were active, the duration of the entire eruption of a typical Wapshilla Ridge flow could have been longer than 3–4 years.

[36] The local eruption rate in the Maxwell Lake dike would have been at the lower end of our estimated range if basalt flow were intermittent rather than continuous. If flow were intermittent, then 3–4 years is a minimum estimate of dike longevity. Varying discharge rates are well documented in basaltic eruptions, typically with a high initial rate of magma discharge waning over the duration of the eruption [*Wadge*, 1981], which is consistent with the basalt flux calculated from the advective transport simulations (Figure 10a). Physical evidence for intermittent discharge during CRBG eruptions has been documented at the vent for the Joseph Creek flow of the Grande Ronde Basalt [*Reidel and Tolan*, 1992]. While we cannot preclude some pauses during flow in this dike, the lack of internal contacts as well as the regular textural progression across the Maxwell Lake dike and wall rock melt zones is more consistent with continuous (and likely waning) flow and a single cooling history.

[37] Volumetric eruption rates calculated on the basis of our thermal models for a typical Wapshilla Ridge flow are within the range reported for other CRBG eruptions (Table 3). Our minimum eruption rates, calculated from the advective transport simulations, are comparable to rates estimated from slow emplacement models for the Roza flow [*Self et al.*, 1997; *Thordarson and Self*, 1998]. Our maximum eruption rates are an order of magnitude lower than rates calculated using rapid emplacement models [*Swanson et al.*, 1975; *Reidel and Tolan*, 1992] yet an order of magnitude higher than slow emplacement estimates. Wapshilla Ridge eruption rates are similar to the maximum eruption rate of $4300 \text{ m}^3 \text{ s}^{-1}$ reported for the 1783 Laki (Skaftár Fires) eruption, the largest historical fissure eruption [*Thordarson and Self*, 1993]. Although our maximum calculated volumetric eruption rate is consistent with models of rapid flow emplacement, the calculated minimum eruption rates and longevity of the Maxwell Lake dike (3–4 years) support slower emplacement models.

[38] It is commonly observed that within hours of the onset of a fissure eruption, lava fountaining becomes restricted to a few points along the fissure. With continued eruption, lava flow becomes localized to only a few long-lived vents [*Decker*, 1987, and references therein]. *Delaney and Pollard* [1982] and *Bruce and Huppert* [1990] explain this transition as solidification in narrow portions of dikes due to conductive heat loss to the wall rock. As narrow parts of dikes freeze, flow is enhanced in thicker portions, ultimately leading to the development of isolated vents. We propose that this process also explains the presence of wall rock melt zones only along two portions of the Maxwell Lake dike, which experienced higher mass and heat flux as surrounding portions of the dike solidified. In a numerical model, *Quarenì et al.* [2001] showed that the transition from fissure to central vent eruption should

Table 3. Estimates of Eruption Rates for Selected CRBG Flow Units

	Flow Field							
	Generic CRBG	Roza Member	Ice Harbor Member	Teepee Butte Member	Roza Member	Umatilla Member	Sentinel Bluffs Member	Member of Wapshilla Ridge
Flow field volume, km ³	not given	1,500	~7–8	5,000	1,300	720	10,000	~50,000
Flow field areal extent, km ²	not given	40,000	~700	52,000	40,300	15,110	82,461	~100,000
Individual flow volume, km ³	“typical” 100 “large” 1000	700 per cooling unit	0.1 per cooling unit	Limekiln Rapids 840; Joseph Creek 1850; Pruitt Draw, 2350	single eruption	310 approximate	museum 2349; Spokane Falls 777; Stember Creek 1192; California Creek-Airway Heights 1543; McCoy Canyon 4278	~5,000–10,000
Emplacement time	days to weeks	7 days	10 days	days to weeks, maybe months	0.4–4.2 years (individual flows) 6–14 years (flow field)	months	months	3–4 years (individual flow)
Volumetric eruption rate, km ³ d ⁻¹	typical 14–50 large 140–500	1	0.01	tens to hundreds	0.13–0.34	tens to hundreds	tens to hundreds	3–5 ^a 0.1–0.8 ^b
Fissure system length (km)	Not given	~15 wide by ~120 long	~15 wide by ~90 long	70	~5 wide by ~150 long	>50	100	at least 100 long
Eruption rate (km ³ d ⁻¹ km ⁻¹ of fissure)	14 (for fissures >3 m wide)	1	0.0002	>1	0.08 (assuming 4 km active at once)	>1	>1	unknown
Method of eruption rate estimate	numerical model based on rheology arguments; requires turbulent flow	field observations suggesting rapid emplacement and	field observations suggesting rapid emplacement and	assumed rapid emplacement; consistent with field data	numerical model calculating cooling times to form upper crust on flows	evaluation of field data, chemical composition implications with respect to cooling calculations	evaluation of field data, chemical composition implications with respect to cooling calculations	assumes Maxwell Lake dike fed flow for 3–4 years; minimum flux (advective transport model) this paper, <i>Petcovic and Grunder</i> [2003]
Reference(s)	<i>Shaw and Swanson</i> [1970]	<i>Swanson et al.</i> [1975]	<i>Swanson et al.</i> [1975]	<i>Reidel and Tolan</i> [1992]	<i>Self et al.</i> [1997] and <i>Thordarson and Self</i> [1998]	<i>Reidel</i> [1998]	<i>Reidel</i> [2005]	

^aAssumes Maxwell Lake dike fed flow for 3–4 years.

^bMinimum flux (advective transport model).

induce wall rock melting. Wall rock melt zones adjacent to the Maxwell Lake dike provide evidence for the existence of long-lived point sources in flood basalt eruptions.

6. Conclusions

[39] Partially melted wall rock at the margins of the Maxwell Lake dike provide a record of thermal events during eruption and emplacement of Wapshilla Ridge flows of the Grande Ronde Basalt. Two suites of thermal models, static conduction simulations and advective transport simulations, were used to investigate the development of these wall rock melt zones as a consequence of basalt intrusion and flow. Results of static conduction modeling constrained by our field example confirm that simple injection followed by stagnation and cooling was incapable of producing wall rock melt. Whereas the repeated injection scenario generated wall rock melt zones comparable to those observed, the regular textural progression across the dike and its wall rock is inconsistent with repeated brittle injection. Instead, static conduction results suggest that sustained flow for 3–4 years caused development of the melt zones observed in the dike.

[40] Magma flow in the dike and development of wall rock melt zones were further investigated via advective transport modeling. These simulations produced an initial centerline velocity of $\sim 10 \text{ m s}^{-1}$ in the dike. Up to $\sim 1 \text{ m}$ thick solidified basalt margins developed shortly after flow was initiated, causing constriction of the dike and a rapid decay in magma velocity during the first 60 days of flow. After the initial solidification, continued flow produced a small amount of melting in the solidified dike margin, causing the basalt flux to increase slightly and the centerline velocity to remain relatively stable at 2 m s^{-1} for the duration of flow. Wall rock melting was initiated after 320–380 days of flow, and the wall rock had dropped below its solidus temperature within 2 years after flow ceased. The thickness, distribution, and fractions of wall rock melt zones produced by this model closely approximate our field observations.

[41] Maximum eruption rates for CRBG flows, based on the assumption that the Maxwell Lake dike fed a typical Wapshilla Ridge flow, range from 3 to $5 \text{ km}^3 \text{ d}^{-1}$, an order of magnitude greater than rates calculated for the Roza CRBG flow and the maximum eruption rate during the Laki 1783 fissure eruption. Local eruption rates could have been lower if mass flux through the dike waned during eruption, if the dike were intermittently active, or if other fissure segments fed the same flow. Conversion of the advective transport model output yields an initial flux of basalt in the dike of $0.8 \text{ km}^3 \text{ d}^{-1}$ waning rapidly to $0.1 \text{ km}^3 \text{ d}^{-1}$, which is consistent with observed Hawaiian-style fissure eruptions. Lower local eruption rates require that additional fissure segments (as yet unidentified) fed the same flow, and may indicate that the duration of the entire eruption was longer than 3–4 years.

[42] Model results suggest that the Maxwell Lake dike sustained high magma flux for at least several years. The transition from fissure eruption to localized vents during basaltic volcanism is often explained as a function of cooling in narrow portions of dikes coupled with enhanced flow in thicker portions, resulting in isolated, long-lived

vents. We propose that the Maxwell Lake dike represents an upper crustal ($\sim 2 \text{ km}$) exposure of a long-lived point source for the CRBG and serves as a model for identifying other such sources in other flood basalts.

[43] **Acknowledgments.** We thank Anita Grunder and George Bergantz for their assistance with interpretation of the model and field data. Steve Reidel provided distribution data, flow volume estimates, and compositional data for the member of Wapshilla Ridge. Bill Taubeneck conducted the original mapping and directed us to the Maxwell Lake dike field location. Comments by and discussions with Anita Grunder, Steve Reidel, and John Dilles enhanced this manuscript. We are grateful to Laszlo Keszthelyi, Larry Mastin, and an anonymous reviewer for their insightful comments that greatly improved this manuscript. This research has been partially supported by a NASA Earth Systems Science Graduate Fellowship (J.D.).

References

- Baksi, A. K. (1989), Reevaluation of the timing and duration of extrusion of the Innaha, Picture Gorge, and Grande Ronde Basalts, Columbia River Basalt Group, in *Volcanism and Tectonism in the Columbia River Flood-Basalt Province*, edited by S. P. Reidel and P. R. Hooper, *Spec. Pap. Geol. Soc. Am.*, 239, 105–111.
- Barboza, S. A., and G. W. Bergantz (1996), Dynamic model of dehydration melting motivated by a natural analogue: Applications to the Ivrea-Verbano zone, northern Italy, *Trans. R. Soc. Edinburgh*, 87, 23–31.
- Bergantz, G. W. (1990), Melt fraction diagrams: The link between chemical and transport models, in *Modern Methods of Igneous Petrology: Understanding Magmatic Processes*, *Rev. Mineral. Geochem.*, vol. 24, edited by J. Nicholls and J. K. Russell, pp. 240–257, Mineral. Soc. of Am., Washington, D. C.
- Bruce, P., and H. Huppert (1990), Solidification and melting along dykes by laminar flow of basaltic magma, in *Magma Transport and Storage*, edited by M. Ryan, pp. 87–102, John Wiley, New York.
- Camp, V. E., and M. E. Ross (2004), Mantle dynamics and the genesis of mafic magmatism in the Pacific Northwest, *J. Geophys. Res.*, 109, B08204, doi:10.1029/2003JB002838.
- Camp, V. E., M. E. Ross, and W. E. Hanson (2003), Genesis of flood basalts and Basin and Range volcanic rocks from Steens Mountain to the Malheur River Gorge, Oregon, *Geol. Soc. Am. Bull.*, 115, 105–128.
- Decker, R. W. (1987), Dynamics of Hawaiian volcanoes, an overview, in *Volcanism in Hawaii*, edited by R. W. Decker, T. L. Wright, and P. H. Stauffer, *U.S. Geol. Surv. Prof. Pap.*, 1350(2), 997–1018.
- Delaney, P. T. (1987), Heat transfer during emplacement and cooling of mafic dykes, in *Mafic Dyke Swarms*, edited by H. C. Halls and W. L. F. Fabrig, *Geol. Assoc. Can. Spec. Pap.*, 34, 31–46.
- Delaney, P. T., and D. D. Pollard (1982), Solidification of basaltic magma during flow in a dike, *Am. J. Sci.*, 282, 856–885.
- Dingwell, D. B., et al. (1993), Magma rheology, in *Handbook on Experiments at High Pressure and Applications to the Earth's Mantle*, edited by R. W. Luth, *Short Course Handb. Mineral. Assoc. Can.*, 21, 131–196.
- Dobran, F. (1992), Nonequilibrium flow in volcanic conduits and application to the eruptions of Mt. St. Helens on May 18, 1980, and Vesuvius in AD 79, *J. Volcanol. Geotherm. Res.*, 49, 285–311.
- Dobran, F. (2001), *Volcanic Processes, Mechanisms in Material Transport*, 590 pp., Springer, New York.
- Dufek, J. D. (2004), Lower crustal magma genesis and preservation: A stochastic framework for the evaluation of basalt-crust interaction, M.S. thesis, Univ. of Washington, Seattle.
- Dufek, J. D., and G. W. Bergantz (2005), Lower crustal magma genesis and preservation: A stochastic framework for the evaluation of basalt-crust interaction, *J. Petrol.*, doi:10.1093/petrology/egi049.
- Fialko, Y. A., and A. M. Rubin (1999), Thermal and mechanical aspects of magma emplacement in giant dike swarms, *J. Geophys. Res.*, 104, 23,033–23,049.
- Ghiorso, M. S., and R. O. Sack (1995), Chemical mass transfer in magmatic processes: IV: A revised and internally consistent thermodynamic model for the interpolation and extrapolation of liquid-solid equilibria in magmatic systems at elevated temperatures and pressures, *Contrib. Mineral. Petrol.*, 119, 197–212.
- Gibson, I. L. (1969), A comparative account of the flood basalt volcanism of the Columbia Plateau and eastern Iceland, *Bull. Volcanol.*, 33, 420–437.
- Grunder, A. L., and W. H. Taubeneck (1997), Partial melting of tonalite at the margins of Columbia River Basalt Group dikes, Wallowa Mountains, Oregon, *Geol. Soc. Am. Abstr. Prog.*, 29, 18.

- Ho, A. M., and K. V. Cashman (1997), Temperature constraints on the Ginkgo flow of the Columbia River Basalt Group, *Geology*, **25**, 403–406.
- Hon, K., J. Kauhikaua, R. Denlinger, and K. MacKay (1994), Emplacement and inflation of pahoehoe sheet flows: Observations and measurements of active lava flows on Kilauea Volcano, Hawaii, *Geol. Soc. Am. Bull.*, **106**, 351–370.
- Hooper, P. R. (1985), A case of simple magma mixing in the Columbia River Basalt Group; the Wilbur Creek, Lapwai, and Asotin flows, Saddle Mountains Formation, *Contrib. Mineral. Petrol.*, **91**, 66–73.
- Hooper, P. R. (2000), Chemical discrimination of Columbia River basalt flows, *Geochem. Geophys. Geosyst.*, **1**(6), doi:10.1029/2000GC000040.
- Hooper, P. R., and C. J. Hawkesworth (1993), Isotopic and geochemical constraints on the origin and evolution of the Columbia River Basalt, *J. Petrol.*, **34**, 1203–1246.
- Hooper, P. R., and S. P. Reidel (1989), Dikes and vents feeding the Columbia River basalt, in *Geologic Guidebook for Washington and Adjacent Area*, edited by N. L. Joseph et al., *Inf. Circ. Wash. Div. Geol. Earth Resour.*, **86**, 255–273.
- Huppert, H. E., and R. S. J. Sparks (1989), Chilled margins in igneous rocks, *Earth Planet. Sci. Lett.*, **92**, 397–405.
- Keszthelyi, L., and S. Self (1998), Some physical requirements for the emplacement of long basaltic lava flows, *J. Geophys. Res.*, **103**, 27,447–27,464.
- Kitchen, D. E. (1989), The disequilibrium partial melting and assimilation of Caledonian granite by Tertiary basalt at Barnesmore, Co. Donegal, *Geol. Mag.*, **126**, 397–405.
- Mangan, M. T., T. L. Wright, D. A. Swanson, and G. R. Byerly (1986), Regional correlation of Grande Ronde Basalt flows, Columbia River Basalt Group, Washington, Oregon, and Idaho, *Geol. Soc. Am. Bull.*, **97**, 1300–1318.
- Marsh, B. D. (1981), On the crystallinity, probability of occurrence, and rheology of lava and magma, *Contrib. Mineral. Petrol.*, **78**, 85–98.
- Petcovic, H. L. (2000), Partial melting of tonalite at the margins of a Columbia River Basalt Group dike, Wallowa Mountains, northeastern Oregon, M.S. thesis, Oregon State Univ., Corvallis.
- Petcovic, H. L., and A. L. Grunder (2003), Textural and thermal history of partial melting in tonalitic wallrock at the margin of a basalt dike, Wallowa Mountains, Oregon, *J. Petrol.*, **44**, 2287–2312.
- Petford, N., and K. Gallagher (2001), Partial melting of mafic (amphibolitic) lower crust by periodic influx of basaltic magma, *Earth Planet. Sci. Lett.*, **193**, 483–499.
- Philpotts, A. R., and P. M. Asher (1993), Wallrock melting and reaction effects along the Higganum diabase dike in Connecticut: Contamination of a continental flood basalt feeder, *J. Petrol.*, **34**, 1029–1058.
- Piwinski, A. J., and P. J. Wyllie (1968), Experimental studies of igneous rock series; a zoned pluton in the Wallowa Batholith, Oregon, *J. Geol.*, **76**, 205–234.
- Pope, S. B. (2000), *Turbulent Flows*, Cambridge Univ. Press, New York.
- Price, S. A. (1977), An evaluation of dike-flow correlations indicated by geochemistry, Chief Joseph swarm, Columbia River Basalt, Ph.D. Thesis, Univ. of Idaho, Pocatello.
- Quarenii, F., G. Ventura, and F. Mulargia (2001), Numerical modeling of the transition from fissure- to central-type activity on volcanoes: A case study from Salina Island, Italy, *Phys. Earth Planet. Inter.*, **124**, 213–221.
- Reidel, S. P. (1998), Emplacement of Columbia River flood basalt, *J. Geophys. Res.*, **103**, 27,393–27,410.
- Reidel, S. P. (2005), A lava flow without a source: The Cohasset flow and its compositional components, Sentinel Bluffs Member, Columbia River Basalt Group, *J. Geol.*, **113**, 1–21.
- Reidel, S. P., and K. R. Fecht (1987), The Huntzinger flow: Evidence of surface mixing of the Columbia River Basalt and its petrogenetic implication, *Geol. Soc. Am. Bull.*, **98**, 664–677.
- Reidel, S. P., and T. L. Tolan (1992), Eruption and emplacement of flood basalt: An example from the large-volume Teepee Butte Member, Columbia River Basalt Group, *Geol. Soc. Am. Bull.*, **104**, 1650–1671.
- Reidel, S. P., T. L. Tolan, P. R. Hooper, M. H. Beeson, K. R. Fecht, R. D. Bentley, and J. L. Anderson (1989), The Grande Ronde Basalt, Columbia River Basalt Group: Stratigraphic descriptions and correlations in Washington, Oregon, and Idaho, in *Volcanism and Tectonism in the Columbia River Flood-Basalt Province*, edited by S. P. Reidel and P. R. Hooper, *Spec. Pap. Geol. Soc. Am.*, **239**, 21–53.
- Rodi, W. (1984), *Turbulence Models and Their Application in Hydraulics, A State of the Art Review*, Int. Assoc. for Hydraul. Res., Delft, Netherlands.
- Ross, M. E. (1983), Chemical and mineralogical variations within four dikes of the Columbia River Basalt Group, southeastern Columbia Plateau, *Geol. Soc. Am. Bull.*, **94**, 1117–1126.
- Scaillet, B., F. Holtz, and M. Pichivant (1998), Phase equilibrium constraints on the viscosity of silicic magmas: 1. Volcanic-plutonic comparison, *J. Geophys. Res.*, **103**, 27,257–27,266.
- Self, S., T. Thordarson, L. Keszthelyi, G. P. L. Walker, K. Hon, M. T. Murphy, P. Long, and S. Finnemore (1996), A new model for the emplacement of Columbia River basalts as large, inflated pahoehoe lava flow fields, *Geophys. Res. Lett.*, **23**, 2689–2692.
- Self, S., T. Thordarson, and L. Keszthelyi (1997), Emplacement of continental flood basalt lava flows, in *Large Igneous Provinces: Continental, Oceanic, and Planetary Flood Volcanism*, *Geophys. Monogr. Ser.*, vol. 100, edited by J. J. Mahoney and M. F. Coffin, pp. 381–410, AGU, Washington, D. C.
- Shaw, H. R. (1972), Viscosities of magmatic liquids: An empirical method of prediction, *Am. J. Sci.*, **272**, 870–893.
- Shaw, H. R., and D. A. Swanson (1970), Eruption and flow rates of flood basalts, in *Proceedings of the Second Columbia River Basalt Symposium*, edited by E. H. Gilmour and D. Stradling, pp. 271–299, East. Wash. State Coll. Press, Cheney.
- Swanson, D. A., and T. L. Wright (1981), Guide to geologic field trip between Lewiston, Idaho, and Kimberly, Oregon, emphasizing the Columbia River Basalt Group, in *Guides to Some Volcanic Terranes in Washington, Idaho, Oregon, and Northern California*, edited by D. A. Johnston and J. Donnelly-Nolan, *U.S. Geol. Surv. Circ.*, **838**, 1–28.
- Swanson, D. A., T. L. Wright, and R. T. Heltz (1975), Linear vent systems and estimated rates of magma production and eruption for the Yakima Basalt on the Columbia Plateau, *Am. J. Sci.*, **275**, 877–905.
- Taubeneck, W. H. (1970), Dikes of Columbia River Basalt in northeastern Oregon, western Idaho, and southeastern Washington, in *Proceedings of the Second Columbia River Basalt Symposium*, edited by E. H. Gilmour and D. Stradling, pp. 73–96, East. Wash. State Coll. Press, Cheney.
- Taubeneck, W. H., and R. A. Duncan (1997), Preferential occurrence of eruptive axes of dikes of the Columbia River Basalt Group in unmetamorphosed Mesozoic granitic intrusives, with $^{40}\text{Ar}/^{39}\text{Ar}$ dates for four dikes and two of the earliest flows of basalt, northeast Oregon and western Idaho, *Geol. Soc. Am. Abstr. Programs*, **29**, 48.
- Tolan, T. L., S. P. Reidel, M. H. Beeson, J. L. Anderson, K. R. Fecht, and D. A. Swanson (1989), Revisions to the estimates of the areal extent and volume of the Columbia River Basalt Group, in *Volcanism and Tectonism in the Columbia River Flood-Basalt Province*, edited by S. P. Reidel and P. R. Hooper, *Spec. Pap. Geol. Soc. Am.*, **239**, 1–20.
- Thordarson, T., and S. Self (1993), The Laki (Skaftár Fires) and Grímsvötn eruptions in 1783–1785, *Bull. Volcanol.*, **55**, 233–263.
- Thordarson, T., and S. Self (1998), The Roza Member, Columbia River Basalt Group: A gigantic pahoehoe lava flow field formed by endogenous processes?, *J. Geophys. Res.*, **103**, 27,411–27,445.
- Touloukian, Y. S., W. R. Judd, and R. F. Roy (Eds.) (1981), *Physical Properties of Rocks and Minerals*, McGraw-Hill, New York.
- Wadge, G. (1981), The variation of magma discharge during basaltic eruptions, *J. Volcanol. Geotherm. Res.*, **11**, 139–168.

J. D. Dufek, Department of Earth and Space Sciences, University of Washington, Box 351310, Seattle, WA 98195-1310, USA. (dufek@u.washington.edu)

H. L. Petcovic, Department of Geosciences, Western Michigan University, 1187 Rood Hall, Kalamazoo, MI 49008, USA. (heather.petcovic@wmich.edu)